Journal of Inorganic Biochemistry 199 (2019) 110759

Contents lists available at ScienceDirect

Journal of Inorganic Biochemistry

journal homepage: www.elsevier.com/locate/jinorgbio

The copper(II) binding centres of carbonic anhydrase are differently affected by reductants that ensure the redox intracellular environment

Giovanni Tabbì[a], Antonio Magrì[a], Enrico Rizzarelli[a,b,c,*]

[a] Institute of Crystallography, National Council of Research, CNR, S.S. Catania, via P. Gaifami 18, Catania, Italy
[b] Department of Chemical Sciences, University of Catania, Viale A. Doria 6, Catania, Italy
[c] Consorzio Interuniversitario per la Ricerca dei Metalli nei Sistemi Biologici, Via Ulpiani 27, Bari, Italy

ABSTRACT

Copper is involved in several biological processes. The static and labile copper pools are controlled by means of a network of influx and efflux transporters, storage proteins, chaperones, transcription factors and small molecules as glutathione (GSH), which contributes to the cell reducing environment. To follow the fate of intracellular copper labile pool, a variant of human apocarbonic anhydrase has been proposed as fluorescent probe to monitor cytoplasmic Cu^{2+}. Aware that in this cellular compartment copper ion is present as Cu^{+}, electron spin resonance technique (ESR) was used to ascertain whether (bovine or human) carbonic anhydrase (CA) was able to accommodate Cu^{+} in the same sites occupied by Cu^{2+}, in the presence of naturally occurring reducing agents such as ascorbate and GSH. Our ESR results on Cu^{2+} complexes with CA allow for a complete characterization of the two metal binding sites of the protein in solution. The use of the reported affinity constants of zinc in the catalytic site and of Cu^{2+} in the peripheral and catalytic site, allow us to obtain the speciation of copper species mimicking the spectroscopic study conditions. The different Cu^{2+} coordination features in the catalytic and the peripheral (the N-terminus cleft mouth) binding sites influence the chemical reduction effect of the two main naturally occurring reductants. Ascorbate reversibly reduces the Cu^{2+} complex with CA, while glutathione irreversibly induces the formation of Cu^{2+} complex with its oxidized form (GSSG). Our results questioned the use of CA as intracellular Cu^{2+} sensor. Furthermore, translating these findings to intracellular environment, the conversion of GSH in GSSG can significantly alter the metallostasis.

1. Introduction

Copper is an essential metal ion for life [1,2]. This d-block metal ion is largely present in enzymes and is involved in several biological processes, including respiration, protection from oxidative stress, homeostasis for the growth, brain functioning and signal transduction [3–5]. Copper dyshomeostasis, therefore, could result in different diseases, including neurodegeneration, cancer and diabetes [6–10].

To avoid copper distribution and homeostasis alteration, a cellular network is employed to regulate both: i) the static pool, that comprises the metal ion tightly bound to proteins and enzymes and ii) the labile pool, that consists of weakly bound metal ion. These two copper pools are controlled by means of influx and efflux transporters, storage proteins, chaperones, transcription factors and small molecules as reduced glutathione (GSH) that also contributes to the cell reducing environment [11]. GSH, which is present at millimolar concentrations in cells [12,13], would also maintain copper in the reduced state; Cu^{+}-GSH complexes have been reported to be stable even in the presence of oxygen for a short time [14], and act as exchangeable cytosolic copper pool, transferring it to chaperones, metallothioneins and enzymes [15].

Selective fluorescent small-molecule probes and genetically encoded biosensors have been developed, allowing for the determination of labile copper with spatial-temporal resolution. Due to the reducing environment in eukaryotic cells, the majority of intracellular labile copper exists as Cu^{+}. Copper sensors for cell imaging are therefore designed to target specifically Cu^{+} over Cu^{2+}, in addition to the selectivity against other common transition metals [16–19]. However, small molecule one- and two-photon sensors for Cu^{2+} bioimaging and genetically encoded copper probes have been described [19–23]. Among the genetically encoded protein-based sensors McCranor et al. [24] used a variant of human apocarbonic anhydrase II (apo*h*CA II), which could monitor cellular copper(II) ions via fluorescence lifetime imaging microscopy (FLIM). The human C206S L198C Q92A CA II variant exhibited 25-fold higher selectivity for Cu^{2+} over Zn^{2+} than the wild type protein, overcoming Zn^{2+} interference. The authors claimed that: “In view of the rather different geometry of protein Cu(I) binding sites compared with Cu(II) sites, it seems unlikely that the Q92A variant will bind Cu(I) with nearly the same affinity as Cu(II), and Cu(I) is unlikely to interfere.”

Carbonic anhydrase (holoenzyme CA) is a well-characterized zinc metalloenzyme, which catalyzes the reversible conversion of water and carbon dioxide to a bicarbonate ion and proton; the active site of this enzyme, located at the bottom of a deep cleft [25], contains zinc(II) ion bound to three histidines (His) and a water or hydroxide ion in a

* Corresponding author at: Institute of Crystallography, National Council of Research, CNR, S.S. Catania, via P. Gaifami 18, Catania, Italy.
E-mail address: erizzarelli@unict.it (E. Rizzarelli).

https://doi.org/10.1016/j.jinorgbio.2019.110759
Received 5 April 2019; Received in revised form 18 June 2019; Accepted 1 July 2019
Available online 03 July 2019
0162-0134/

distorted tetrahedral geometry [26–28].

Many derivatives of bovine or human carbonic anhydrase II (holoenzyme *b/h*CA II), in which the zinc(II) ion has been substituted with other metal ions like Co^{2+}, Ni^{2+}, Cu^{2+}, Ag^{+}, Hg^{2+}, etc. [29], have been prepared and characterized. The metals have been found to replace Zn(II) in the active site. Differently from the others, Cu(II) binds the enzyme in a 2:1 stoichiometric ratio, both in solution [30] and in the solid state [31]. The X-ray structure of Cu_2*h*CA II [31] shows a copper(II) ion binding site at the mouth of the active site cleft [32,33] involving two histidines, His4 and His64 and four water molecules in a pseudo-octahedral geometry. The copper(II) ion in the active site of *h*CA II, conversely, experiences a pentacoordinated geometry involving the binding of His94 in apical position and four ligands, His96, His119, H_2O and O_2, essentially in a plane. The coordination environment at the mouth of the active site cleft could favor digonal Cu^{+} complex in a 2-coordinated species $[Cu(His)_2]^{+}$ as reported for Cu^{+} bound to human serum albumin (HSA) [34]. Cu^{2+}-HSA complex can be reduced to form stable Cu^{+}-HSA species under both anaerobic and aerobic conditions [35,36]. Furthermore, the Cu^{+} affinity for HSA is more than two orders of magnitude greater than that reported for Cu^{2+} determined under similar experimental conditions [34]. Analogous Cu^{+} coordination environment characterizes the β-amyloid peptide (Aβ) and the prion protein octarepeat [37,38]. Cu^{+} bound to two histidine residues in Aβ is not oxidized by the presence of O_2 [39,40].

This scenario prompted us to ascertain whether CA was able to accommodate Cu^{+} in the same sites occupied by Cu^{2+}, in the presence of naturally occurring reducing agents such as ascorbic acid (Asc) and GSH, having $E^0 = +0.051$ V and $E^0 = -0.228$ V, respectively [41].

Since the early seventies, electron spin resonance (ESR) measurements have been carried out to characterize the Cu^{2+} binding features at the catalytic site, mainly to assign the number of the histidine residues involved in the metal coordination to bovine and human CAs [42–46].

On the other hand, it is well known that the histidine residues are present in the same sites of the N-terminus cleft domain in the two CA isoforms [47].

Recently, ESR parameters for the copper(II) complexes with human carbonic anhydrase II have been reported for the metal bound both to catalytic and non-catalytic site by the use a recombinant protein [32,33].

The different experimental conditions (pH, buffer, temperature, metal to ligand ratios, starting protein, etc.) can explain some contrasting results. Therefore, ESR measurements were performed to determine the magnetic parameters of the different copper(II) complexes with bovine and human CA in our experimental conditions. The $g_{||}$ and $A_{||}$ values allowed us to follow the fate of the metal species in the presence of a large excess of reductants (Asc and GSH) at different times.

The possible formation of Cu(I) complexes with *h/b*CA II in cell-free conditions can open a new scenario about the use of protein-based sensors of copper in cellular environment.

2. Experimental

In all experiments ultrapure water (Milli-Q H_2O, 25 °C, 18.2 MΩ·cm^{-1}) was employed.

2.1. Bovine copper(II)-CA II

Cu_2*b*CA II was prepared by adding more than one equivalent of $CuSO_4$ to the apo*b*CA II dissolved in 10 mM Tris (tris(hydroxymethyl) aminomethane, Sigma-Aldrich) buffer (pH 7.5 and 10 mM Na_2SO_4). A concentration of 5.7×10^{-4} M of Cu_2*b*CA II was evaluated by UV–Vis spectroscopy ($\varepsilon_{780} = 138\ M^{-1}\ cm^{-1}$, $\varepsilon_{738} = 151\ M^{-1}\ cm^{-1}$).

2.2. Human holoenzyme of CA II

Holoenzyme of human carbonic anhydrase (*h*CA II) was purchased from Sigma-Aldrich (product code C6165, lot no. 078K6276, enzymatic activity measured by Sigma-Aldrich in the certificate analysis: 5563 Wilbur-Anderson units/mg protein) and used without further purification; it was dissolved in 10 mM Tris or MOPS (4-morpholinepropanesulfonic acid, Sigma) buffer at pH 7.5. The *h*CA II was employed in a concentration range of $1–6 \times 10^{-4}$ M.

2.3. Human Cu_2CA II

Cu_2*h*CA II was obtained by adding more than two equivalents of $Cu(NO_3)_2$ to the human holoenzyme (1×10^{-4} M) in Tris buffer (10 mM) at pH 7.5.

In order to ascertain the competitive coordination ability of the non-innocent buffers used in the experiments, frozen ESR spectra were run on solutions containing $^{63}Cu(NO_3)_2$ (0.5–0.63 mM) and Tris (10 mM or 50 mM).

2.4. Electron spin resonance

A Bruker Elexsys E500 CW-ESR spectrometer driven by a PC running XEpr program under Linux and equipped with a Super-X microwave bridge operating at 9.3–9.5 GHz, and a SHQE probehead was used throughout this work. All frozen solution ESR spectra of copper(II) complexes were recorded at 150 K by means of an ER4131VT variable temperature apparatus. Copper protein samples were added of a small amount of glycerol (up to 10%) in order to increase spectral resolution. Parallel spin Hamiltonian parameters were taken directly from the experimental spectra, always calculating them from the 2nd and 3rd line to get rid of errors coming from second order effects [48]. Naturally occurring copper contains is a mixture of ^{63}Cu and ^{65}Cu isotopes which possess slightly different hyperfine constants [49]. An improved resolution of the ESR spectra [44] was obtained with the use of isotopically pure $^{63}Cu^{2+}$. In order to achieve a better determination of the magnetic parameters, the experimental spectra were simulated by the program Monoclin [50] (which is able to discriminate one or more species). Instrumental settings of frozen solution ESR spectra were as follow: number of scans 2–10; microwave frequency 9.344–9.376 GHz; modulation frequency 100 kHz; modulation amplitude 0.7 mT; time constant 327 ms; sweep time 2.8 min; microwave power 20 mW; receiver gain 60 dB.

2.5. UV–visible spectroscopic measurements

Optical absorption spectra in the UV–Vis region were recorded at room temperature with a UV–Vis-NIR Jasco V-670 spectrophotometer.

2.6. Chemical reduction

Chemical reduction of the Cu_2*b*CA II 0.57 mM by Asc 2 mM and Cu_2*h*CA II 0.1 mM by GSH 2 mM was monitored by the change in intensity of the ESR signals with time. Immediately following addition of the reductant, samples were transferred to a quartz tube and X-band (9.45 GHz) continuous-wave ESR spectra were obtained at 150 K at different times. The Cu^{2+} signal was quantified using the double integral of the spectrum intensity.

3. Results and discussion

The crystal structure of the Zn,Cu(II)-*h*CA II has been reported showing that Cu^{2+} binds His64 and His4 at a distance of 2.1 Å and 2.0 Å respectively; two water molecules complete the coordination sphere around the metal ion at a distance of 2.2 Å. Two other water molecules are at a distance of 2.5 and 2.8 Å from the Cu^{2+} that

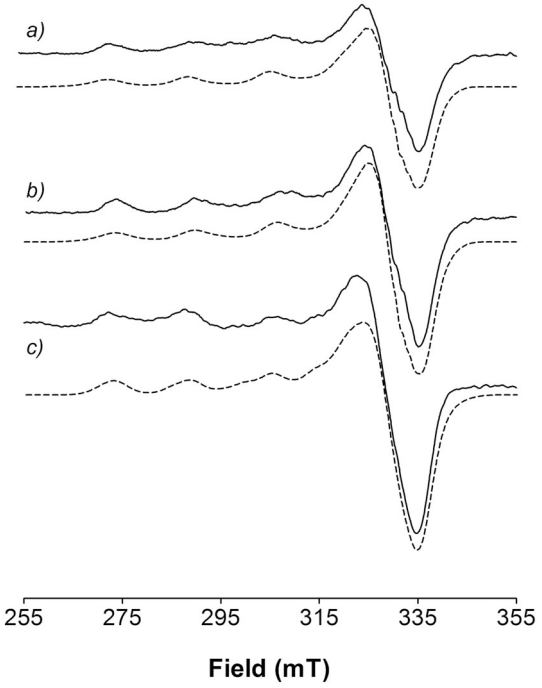

Fig. 1. ESR spectra at 150 K of human holoenzyme (1×10^{-4} M) in buffer solution (Tris 10 mM, pH 7.5) to which were added increased amounts of $^{63}Cu(NO_3)_2$ 1 mM, a) 0.9 eq Cu^{2+}; b) 1.0 eq Cu^{2+}; c) 2.0 eq Cu^{2+}. Simulated spectra are showed in dashed line.

experiences a distorted octahedral coordination geometry. In the active site, a dioxygen molecule is coordinated to the zinc ion that completes its tetrahedral coordination geometry by His94, His96 and His119 binding [51].

In order to have more details on copper(II) binding in solution, we added increasing amounts of $^{63}Cu^{2+}$ to the human holoenzyme. The ESR spectrum recorded at pH 7.5 (Tris buffer, 10 mM) at sub-stoichiometric ratios indicates the formation of one species only; the Hamiltonian parameters calculated for this species are $g_{||} = 2.280$ and $A = 164 \times 10^{-4}$ cm^{-1} (Fig. 1a).

The spectrum remains practically unchanged roughly up to one equivalent of copper (Fig. 1b). However, well beyond one equivalent the addition of copper(II) causes a change in the ESR spectrum. The addition of two equivalents results in the formation of a second species that is readily detected in the ESR spectrum. The simulation of the

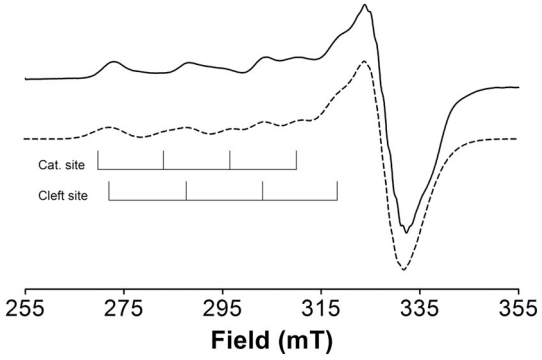

Fig. 2. ESR spectra of Cu_2*b*CA II system (5.7×10^{-4} M) in Tris (10 mM, pH 7.5) (experimental spectrum, solid line; simulated spectrum, dashed line).

spectrum obtained with excess copper(II) yields the following parameters for this second species: $g_{||} = 2.303$ and $A_{||} = 152 \times 10^{-4}$ cm^{-1} (Table 1).

As previously mentioned, the structure of Cu_2*h*CA II has been solved and the ligands involved in the two metal binding sites have been unveiled [31]. Therefore, ESR measurements of Cu_2*b*CA II solutions obtained by adding more than 1 equivalent of Cu^{2+} to the apoenzyme were carried out; the experimental conditions were the same (buffer, pH and temperature, but Cu^{2+} isotopic mixture) previously employed titrating the human holoenzyme with increasing amount of Cu^{2+} (Fig. 2).

The two sets of Hamiltonian parameters of the two species that form at the same percentage were calculated by simulation: $g_{||} = 2.328$ and $A_{||} = 147 \times 10^{-4}$ cm^{-1} and $g_{||} = 2.280$ and $A_{||} = 160 \times 10^{-4}$ cm^{-1} (Table 1).

Coleman et al. [42,44,46] studied the insertion of Cu^{2+} at sub-stoichiometric ratio in human and bovine CA apoenzyme (Table 1) by means of ESR measurements. The author stressed that, despite extensive dialysis, the presence of small amount of extraneous Cu^{2+} affected the spectrum resolution and the assignment of the number of the histidine residues involved in metal binding. On the basis of the analysis of the superhyperfine lines, Cu^{2+} bound to two [43,44] or three [42,46] imidazole groups has been indicated.

The values of the magnetic parameters attributed to human and bovine copper CA in the catalytic site ranges from 2.289 to 2.320 for $g_{||}$ and from 138 to 161 $\times 10^{-4}$ cm^{-1} for $A_{||}$ (Table 1). The different $g_{||}$ and $A_{||}$ values reported by the same research group [42–46] have been justified invoking different temperatures, the use of pure or mixed

Table 1
Hamiltonian parameters of copper(II) substituted CAs.

System[a]		$g_{||}$	$A_{||}$ $10^4 \times$ cm^{-1}	Buffer	Temperature	Sample[c]	Ref.
^{63}Cu*b*CA B	(site)	2.305	140	Tris 25 mM, pH 8	77 K	apo*b*CA B + ss $^{63}Cu^{2+}$	[44]
^{63}Cu*b*CA	(site)	2.320	144	– (Water)	103 K[b]	apo*b*CA B + ss $^{63}Cu^{2}$	[45]
^{65}Cu*h*CA B	(site)	2.295	161	Tris 25 mM, pH 8	112 K	apo*h*CA B + ss $^{65}Cu^{2+}$	[46]
^{63}Cu*h*CA B	(site)	2.295	152	Tris 25 mM, pH 8	112 K	apo*h*CA B + ss $^{63}Cu^{2+}$	[44]
^{63}Cu*h*CA C	(site)	2.305	138	Tris 25 mM, pH 8	112 K	apo*h*CA C + ss $^{63}Cu^{2+}$	[44]
Cu*h*CA B	(site)	2.320	156	Tris 25 mM, pH 8	77 K	apo*h*CA B + ss Cu^{2}	[42]
^{63}Cu*h*CA B	(site)	2.289	150	Tris 25 mM, pH 8	112 K	apo*h*CA B + ss $^{63}Cu^{2+}$	[43]
^{63}Cu*h*CA C	(site)	2.289	154	Tris 25 mM, pH 8	112 K	apo*h*CA C + ss $^{63}Cu^{2+}$	[43]
Cu_2*rh*CA	(site)	2.326	138	ACES 20 mM, pH 7	21 K	apo*rh*CA + ex Cu^{2+}	[32]
Cu_2*rh*CA	(cleft)	2.190	201	ACES 20 mM, pH 7	21 K	apo*rh*CA + ex Zn^{2+} + ss Cu^{2+}	[32]
Cu_2*b*CA II	(site)	2.328 (3)	147 (4)	Tris 10 mM, pH 7.5	150 K	apo*b*CA II + st Cu^{2+}	This work
Cu_2*b*CA II	(cleft)	2.280 (3)	160 (4)	Tris 10 mM, pH 7.5	150 K	apo*b*CA II + st Cu^{2+}	This work
^{63}Cu*h*CA II	(site)	2.303 (3)	152 (4)	Tris 10 mM, pH 7.5	150 K	*h*CA II + ex $^{63}Cu^{2+}$	This work
^{63}Cu*h*CA II	(cleft)	2.280 (3)	164 (4)	Tris 10 mM, pH 7.5	150 K	*h*CA II + ss $^{63}Cu^{2+}$	This work

[a] *b*, bovine, *h*, human, *r*, recombinant. Site stands for Zn catalytic site and cleft for peripheral site.
[b] Hamiltonian parameters calculated from data extrapolated from Fig. 3 of reference [45].
[c] ss – sub-stoichiometric; st – stoichiometric; ex – excess (more than one equivalent).

Table 2
ESR parameters of copper(II) complexes with Tris buffer at physiological pH.

System	$g_{\|\|}$	$A_{\|\|}$, $10^4 \times cm^{-1}$	pH	Note
Cu-Tris	2.231	192	Tris, pH 7.5	Main species
	2.235	188		Minor species

copper isotope and the simulation procedures.

Morpurgo et al. [45] reported the ESR spectra of ^{63}Cu*b*CA in unbuffered aqueous solution of the apoenzyme added of a slightly less stoichiometric copper sulfate. The magnetic parameters (Table 1) $g_{||} = 2.320$ and $A_{||} = 144 \times 10^{-4}\,cm^{-1}$ are in good agreement with those reported in this work and with $g_{||}$ reported by Coleman et al. [42]. Also the Hamiltonian parameters obtained by the use of pure copper isotope, $^{63}Cu^{2+}$, titrating the holoenzyme with more than two equivalents are in good agreement with the data obtained by Coleman et al. [44], adding copper(II) ion to apoenzyme (Table 1). The slight differences compared to our data can be attributed to both the different pH and the effect of the temperature, as previously stressed [43,45]. Further support to this explanation was obtained by ESR measurements carried out on solutions containing copper(II) ion and Tris in the same metal ion to buffer ratios employed by us. The recent accurate studies of Bal et al. [52,53] helped us to assess the speciation of the copper(II) complexes formed by the buffer present in the ESR solution.

The magnetic parameters of the copper(II) complexes with Tris (Table 2) are significantly different from those assigned to the copper (II) insertion in CA, thus allowing us to exclude an alteration of our data due a contribution of copper(II) complexes with Tris.

The recent magnetic parameters of Cu*rh*CA II (*rh* indicates a recombinant human CA II) obtained by Emerson et al. [32] by subtracting the Cu,Zn*rh*CA II data from the Cu_2*rh*CA II spectrum further contributed to the substantial agreement on the ESR parameters pertinent to the copper CA with the metal ion present in the catalytic site (Table 1). While there is reasonable agreement between our data and those reported by Emerson et al. for copper(II) ion present in the catalytic site of enzyme by employing a copper isotope mixture, significant differences appear between the ESR parameters pertinent to copper(II) ion in the mouth of the cleft. On the other hand, it is true that the spectroscopic data have been obtained by the use of a recombinant protein that is characterized by the presence of a methionine residue at position 1 of the natural sequence [54,55]. The added amino acid residue could affect the spectroscopic parameters.

Utilizing isothermal calorimetry (ITC) measurements, reliable intrinsic affinity constants have been reported concerning both the zinc (II) binding at the catalytic site [56] and of copper(II) at the catalytic (C) or at the peripheral binding site (P) [32]. In keeping with the series of Irving and Williams [57] the copper(II) complex at the catalytic binding site showed a higher value of the constant (9.5×10^9) in comparison with that of zinc (2.0×10^9), both resulting lower than that (4.9×10^{12}) of copper bound at mouth of the cleft (the peripheral binding site). These constants were employed to obtain by means of Hyss software [58] the amount of different species (Table 3) formed in the experimental conditions used in the ESR experiments.

The speciation results of the computed titrations shows that the copper(II) ion added at sub-stoichiometric ratio interacts with the binding donor atoms present at the mouth of the cleft alone, while the catalytic site remains completely occupied by zinc (Table 3). Therefore, the recorded ESR spectra refer to the copper complex species present at peripheral site. This species remains the main species in the stoichiometric conditions, while a very small amount of copper(II) ion is present at the catalytic site that is essentially occupied by zinc(II) ions. Finally, at 2:1: Cu(II):*h*CA II ratio, the catalytic site is populated at 69% by copper(II) complex species respect to 31% of zinc(II) complex.

3.1. Chemical reduction

The X-ray structures and the ESR parameters indicate different coordination geometries between the two copper sites. In addiction they differ also for the number of histidine ligands, all these aspects might affect in a different manner their propensity to reduction in aqueous solution.

In order to ascertain the ability of the CA to bind Cu^+, the changes of the ESR spectra of Cu_2*b*CA II were followed by adding a three-fold excess of a reducing agent such as ascorbic acid, whose concentration varies from micromolar in plasma to millimolar in leukocytes [59]. Both copper(II) ions in Cu_2*b*CA II were rapidly reduced to Cu(I) ions after the addition of ascorbic acid. The intensity of the ESR lines decreased of 52% (see Fig. 3), after 8 min from mixing.

This spectrum was simulated employing the same parameter sets of the Cu_2*b*CA II; the percentage of the species with copper(II) ion in the catalytic site was slightly lower than that in which the metal ion occupied the cleft mouth site (40% vs. 60%). After 30 min the spectrum remained practically the same. The metal ion appears more prone to reduction in the catalytic site than in the N-terminus binding site, as expected for Cu^{2+} that experiences a tetrahedrally distorted coordination environment [31,32,45] (N_3O) in the catalytic site. This coordination geometry can favorably accommodate the diamagnetic Cu^+, while in the peripheral site Cu^{2+} is bound to the imidazole nitrogens of two histidine residues and two water molecules that complete a square equatorial coordination plane reaching a pseudo-octahedral geometry with two more distant water molecules. Thus, Cu^+ following the ascorbate action reaches a digonal coordination geometry typical of d^{10} metal ions, but by an energy unfavoured coordination geometry rearrangement.

The reduction processes were reversible; after four days, the copper (I) species were re-oxidized by the dioxygen and the ESR spectrum of the Cu_2*b*CA II resulted perfectly superimposable to the original.

As previously mentioned, glutathione is present in cells predominantly in its reduced form (GSH) at millimolar concentrations [60]. To test the effect of this natural reducing agent on the two copper sites of the protein, GSH (2 mM) was added at 0.1 mM solution of the copper derivative. The ESR spectra (Fig. 4a) showed a prompt reduction of the signal intensity due to reduction of the two cupric species, which remained in the reduced state even 1 h after exposition to the dioxygen (Fig. 4b,c). After one day, the Cu^{2+} ESR signal is fully recovered but this new spectrum is characterized by the following Hamiltonian parameters: $g_{||} = 2.258$ and $A_{||} = 179 \times 10^{-4}\,cm^{-1}$; these parameters are different from those of the starting system (Fig. 4d,e).

Table 3
Computed molar concentration (M) of different complex species formed by *h*CA II and Cu(II) mimicking the experimental conditions of ESR spectra.

Added Cu(II) amount	$[h\text{CA II}]_a$[a]	$[\text{Cu(II)}]_a$[a]	$[h\text{CA II}]_e$[b]	$[\text{Cu(II)-P}]_e$[b]	$[\text{Cu(II)-C}]_e$[b]
Sub-stoichiometric	1.00×10^{-4}	9.00×10^{-5}	9.98×10^{-5}	8.99×10^{-5}	3.80×10^{-9}
Stoichiometric	1.00×10^{-4}	1.00×10^{-4}	9.96×10^{-5}	9.98×10^{-5}	1.71×10^{-7}
Cu(II):*h*CA II ratio 2:1	1.00×10^{-4}	2.00×10^{-4}	3.14×10^{-5}	1.00×10^{-4}	6.86×10^{-5}

[a] $[h\text{CA II}]_a$ = analytical concentration of holoenzyme; $[\text{Cu(II)}]_a$ analytical concentration of Cu(II).
[b] $[h\text{CA II}]_e$ = equilibrium concentration of holoenzyme; $[\text{Cu(II)-P}]_e$ = equilibrium concentration of Cu(II) complex species at peripheral site; $[\text{Cu(II)-C}]_e$ = equilibrium concentration of Cu(II) complex species at catalytic site.

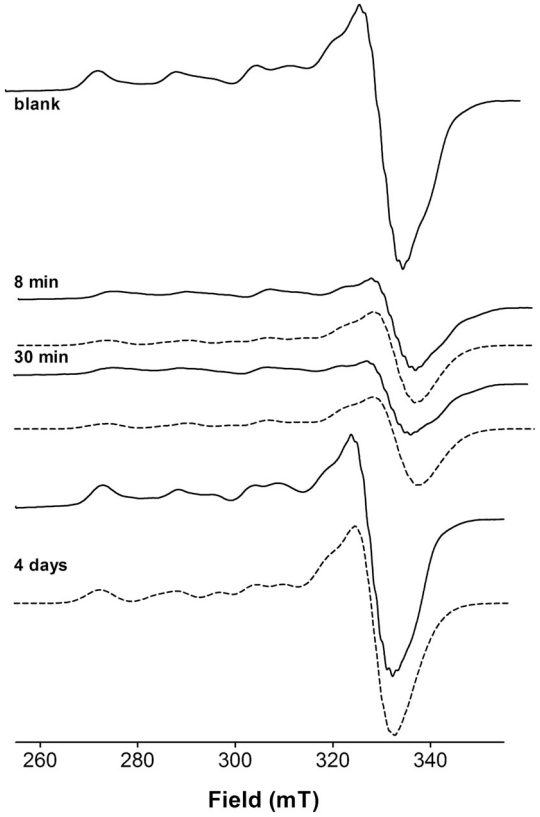

Fig. 3. ESR spectra at 150 K of Cu_2*b*CA II (5.7×10^{-4} M) in Tris buffer (10 mM, pH 7.5) both in the absence (blank) and in the presence of ascorbic acid (2 mM) at different reaction times. Simulated spectra are showed in dashed line.

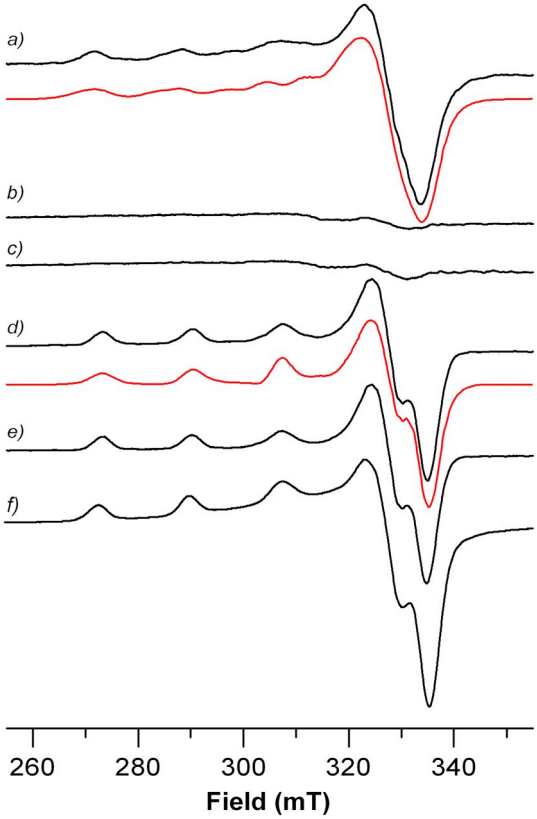

Fig. 4. ESR spectra at 150 K of *h*CA II (0.1 mM) in MOPS (10 mM, pH 7.5) loaded with 2 eq of $^{63}Cu(NO_3)_2$ in the absence (a) and in the presence GSH (2 mM) at different reaction times: (b) 10 min; and in contact with air for (c) 1 h; (d) 1 day; (e) 4 days. (f) ESR spectra at 150 K of a $Cu(NO_3)_2$ solution (0.5 mM) in MOPS (10 mM, pH 7.5) in the presence of GSH (2 mM) left in contact with air for 7 days. Simulated spectra are drawn in red. (For interpretation of the references to colour in this figure legend, the reader is referred to the web version of this article.)

The ESR parameters of Cu-GSSG system (GSSG - oxidized glutathione) have been reported with values, which are quite similar [61–64] ($g_{||} = 2.250$ and $A_{||} = 187 \times 10^{-4}\,cm^{-1}$) to those found after the exposition to dioxygen. This similarity paves the way to a new scenario where the Cu^{2+} initially coordinated by the protein is reduced to Cu(I) but upon re-oxidation the Cu(II) is depleted from the protein forming a stable Cu-GSSG complex.

To better characterize the origin of this last ESR spectrum, Cu^{2+} (natural isotopic abundance, 0.2 mM) was added to a solution of GSH 2 mM in MOPS (10 mM, pH 7.5). This solution was left in contact with air and after a week the obtained ESR spectrum was identical to that reported in the literature, i.e. $g_{||} = 2.251$ and $A_{||} = 187 \times 10^{-4}\,cm^{-1}$ (Fig. 4f), thus supporting the hypothesis that GSH is able to deplete the protein of the two metal ions.

4. Concluding remarks

The results of our ESR study on copper(II) complexes with CA II allow for a complete characterization of the two metal binding sites of the protein in solution. The different copper(II) coordination features between the catalytic and the cleft mouth influence the chemical reduction effect of the two main naturally occurring reductants. Intriguing, the ascorbate induces the formation of the copper(I) complex with CA II in a reversible mode, while the glutathione is able to activate an irreversible redox process and to form a copper(II) complex with GSSG. CA has been proposed as intracellular copper(II) sensor but our results questioned the use of this protein for this aim [24]. Furthermore, translating these findings to intracellular environment, the oxidant process that involves the conversion of GSH in GSSG can significantly alter the metallostasis [17,65]. To ensure redox homeostasis and speciation, copper is transferred by means of GSH from a given chaperone protein to a different protein having a higher affinity [66]; in addition the chaperone redox status is preserved by GSH (the most abundant antioxidant) which, together with its partners, is believed to maintain the redox potential in tissues, cells and individual compartments [67–69]. When GSH is transformed into GSSG, copper chaperone integrity is lost thus perturbing redox and speciation homeostasis [70]. In this scenario, it is imperative that the copper sensor does not alter the status of metallostasis network.

References

[1] H. Tapiero, D.M. Townsend, K.D. Tew, Biomed. Pharmacother. 57 (2003) 386–398.
[2] I. Bertini, H.B. Gray, E.I. Stiefel, J. Selverstone Valentine, Biological Inorganic Chemistry, University Science Books, Mill Valley, CA, USA, Structure and Reactivity, 2007.
[3] S.C. Leary, P.A. Cobine, B.A. Kaufman, G.H. Guercin, A. Mattman, J. Palaty, G. Lockitch, D.R. Winge, P. Rustin, R. Horvath, E.A. Shoubridge, Cell Metab. 5 (2007) 9–20.
[4] S. Masaldan, S.A.S. Clatworthy, C. Gamell, Z.M. Smith, P.S. Francis, D. Denoyer, P.M. Meggyesy, S. La Fontaine, M.A. Cater, Redox Biol. 16 (2018) 322–331.
[5] a) I.F. Scheiber, J.F. Mercer, R. Dringen, Prog. Neurobiol. 116 (2014) 33–57. b) A. Grubman, A.R. White, Expert Rev. Mol. Med. 16 (2014) e11
[6] I. Scheiber, R. Dringen, J.F. Mercer, Met. Ions Life Sci. 13 (2013) 359–387.
[7] G. Pappalardo, D. Milardi, E. Rizzarelli, I. Sovago, The inorganic side of Alzheimer's Disease, in: D. Milardi, E. Rizzarelli (Eds.), Neurodegeneration: Metallostasis and Proteostasis, Royal Society of Chemistry, Cambridge, UK, 2011, pp. 112–140.
[8] R. Giampietro, F. Spinelli, M. Contino, N.A. Colabufo, Mol. Pharm. 15 (2018) 808–820.
[9] V. Barresi, A. Trovato-Salinaro, G. Spampinato, N. Musso, S. Castorina, E. Rizzarelli, D.F. Condorelli, FEBS Open Bio 6 (2016) 794–806.
[10] J. Lowe, R. Taveira-da-Silva, E. Hilário-Souza, IUBMB Life 69 (2017) 255–262.
[11] W. Maret, A. Wedd, Binding, Transport and Storage of Metal Ions in Biological Cells, Royal Society of Chemistry, Cambridge, UK, 2014.

[12] M.M. Schmidt, R. Dringen, Neural metabolism in vivo, in: R. Gruetter, I.Y. Choi (Eds.), Advances in Neurobiology, vol. 4, Springer, New York, USA, 2012, pp. 1029–1050.

[13] a) S.C. Dodani, D.W. Domaille, C.I. Nam, E.W. Miller, L.A. Finney, S. Vogt, C.J. Chang, Proc. Natl. Acad. Sci. U. S. A. 108 (2011) 5980–5985;
b) M.R. Ciriolo, A. Desideri, M. Paci, G. Rotilio, J. Biol. Chem. 265 (1990) 11030–11034;
c) M.R. Ciriolo, A. Battistoni, M. Falconi, G. Filomeni, G. Rotilio, Eur. J. Biochem. 268 (2001) 737–742;
d) D.E. Hartter, A. Barnea, Synapse 2 (1988) 412–415;
e) M.L. Turski, D.C. Brady, H.J. Kim, B.E. Kim, Y. Nose, C.M. Counter, D.R. Winge, D.J. Thiele, Mol. Cell. Biol. 32 (2012) 1284–1295;
f) D.C. Brady, M.S. Crowe, M.L. Turski, G.A. Hobbs, X. Yao, A. Chaikuad, S. Knapp, K. Xiao, S.L. Campbell, D.J. Thiele, C.M. Counter, Nature 509 (2014) 492–496.

[14] a) I. Ascone, A. Longo, H. Dexpert, M.R. Ciriolo, G. Rotilio, A. Desideri, FEBS Lett. 322 (1993) 165–167;
b) A.V. Kachur, C.J. Koch, J.E. Biaglow, Free Radic. Res. 28 (1998) 259–269.

[15] a) J.H. Freedman, R.J. Weiner, J. Peisach, J. Biol. Chem. 261 (1986) 11840–11848;
b) R. Miras, I. Morin, O. Jacquin, M. Cuillel, F. Guillain, E. Mintz, J. Biol. Inorg. Chem. 13 (2008) 195–205.

[16] J.J.A. Cotruvo, A.T. Aron, K.M. Ramos-Torres, C.J. Chang, Chem. Soc. Rev. 44 (2015) 4400–4414.

[17] G. Trusso Sfrazzetto, C. Satriano, G. Tomaselli, E. Rizzarelli, Coord. Chem. Rev. 311 (2016) 125–167.

[18] H.Y. Au-Yeung, C.Y. Chan, K.Y. Tong, Z.H. Yu, J. Inorg. Biochem. 177 (2017) 300–312.

[19] Z. Hao, R. Zhu, P.R. Chen, Curr. Opin. Chem. Biol. 43 (2018) 87–96.

[20] Y. You, Y. Han, Y.M. Lee, S.Y. Park, W. Nam, S.J. Lippard, J. Am. Chem. Soc. 133 (2011) 11488–11491.

[21] H.M. Kim, B.R. Cho, Chem. Rev. 115 (2015) 5014–5055.

[22] H. Wang, B. Fang, L. Zhou, D. Li, L. Kong, K. Uvdal, Z. Hu, Org. Biomol. Chem. 16 (2018) 2264–2268.

[23] M.L. Giuffrida, G. Trusso Sfrazzetto, C. Satriano, S. Zimbone, G. Tomaselli, A. Copani, E. Rizzarelli, Inorg. Chem. 57 (2018) 2365–2368.

[24] B. McCranor, H. Szmacinski, H.H. Zeng, T. Hurst, A. Stoddard, C.A. Fierke, J. Lakowicz, R.B. Thompson, Metallomics 6 (2014) 1034–1042.

[25] a) A. Liljas, K.K. Kannan, P.C. Bergsten, I. Waara, K. Fridborg, B. Strandberg, U. Carlbom, L. Jarup, S. Lovgren, M. Petef, Nat. New Biol. 235 (1972) 131–137;
b) K. Håkansson, M. Carlsson, L.A. Svensson, A. Liljas, J. Mol. Biol. 227 (1992) 1192–1204.

[26] V.M. Krishnamurthy, G.K. Kaufman, A.R. Urbach, I. Gitlin, K.L. Gudiksen, D.B. Weibel, G.M. Whitesides, Chem. Rev. 108 (2008) 946–1051.

[27] H. Vahrenkamp, Dalton Trans. (2007) 4751–4759.

[28] V. Alterio, A. Di Fiore, K. D'Ambrosio, C.T. Supuran, G. De Simone, Chem. Rev. 112 (2012) 4421–4468.

[29] M.G. Lionetto, R. Caricato, M.E. Giordano, T. Schettino, Int. J. Mol. Sci. 17 (2016) 127.

[30] C.A. Di Tusa, T. Christensen, K.A. McCall, C.A. Fierke, E.J. Toone, Biochemistry 40 (2001) 5338–5344.

[31] K. Håkansson, A. Wehnert, A. Lilias, Acta Crystallogr. D Biol. Crystallogr. 50 (1994) 93–100.

[32] H. Song, A.C. Weitz, M.P. Hendrich, E.A. Lewis, J.P. Emerson, J. Biol. Inorg. Chem. 18 (2013) 595–598.

[33] W.L. Nettles, H. Song, E.R. Farquhar, N.C. Fitzkee, J.P. Emerson, Inorg. Chem. 54 (2015) 5671–5680.

[34] M. Sendzik, M.J. Pushie, E. Stefaniak, K.L. Haas, Inorg. Chem. 56 (2017) 15057–15065.

[35] K.L. Haas, A.B. Putterman, D.R. White, D.J. Thiele, K.J. Franz, J. Am. Chem. Soc. 133 (2011) 4427–4437.

[36] L. Perrone, E. Mothes, M. Vignes, A. Mockel, C. Figueroa, M.-C. Miquel, M.-L. Maddelein, P. Faller, ChemBioChem 11 (2010) 110–118.

[37] J. Shearer, V.A. Szalai, J. Am. Chem. Soc. 1330 (2008) 17826–17835.

[38] M.J. Pushie, K.H. Nienaber, A. McDonald, G.L. Millhauser, G.N. George, Chem. Eur. J. 20 (2014) 9770–9783.

[39] R.A. Himes, G.Y. Park, A.N. Barry, N.J. Blackburn, K.D. Karlin, J. Am. Chem. Soc. 129 (2007) 5352–5353.

[40] R.A. Himes, G.Y. Park, G.S. Siluvai, N.J. Blackburn, K.D. Karlin, Angew. Chem. Int. Ed. 47 (2008) 9084–9087.

[41] V.A. Streltsov, R.S.K. Ekanayake, S.C. Drew, C.T. Chantler, S.P. Best, Inorg. Chem. 57 (2018) 11422–11435.

[42] J.S. Taylor, P. Mushak, J.E. Coleman, Proc. Natl. Acad. Sci. 67 (1970) 1410–1416.

[43] J.S. Taylor, J.E. Coleman, J. Biol. Chem. 246 (1971) 7058–7067.

[44] J.S. Taylor, J.E. Coleman, J. Biol. Chem. 248 (1973) 749–755.

[45] L. Morpurgo, G. Rotilio, A. Finazzi Agrò, G. Mondovì, Arch. Biochem. Biophys. 170 (1975) 360–367.

[46] P.H. Haffner, J.E. Coleman, J. Biol. Chem. 250 (1975) 996–1005.

[47] M. Sciaky, N. Limozin, D. Filippi-Foveau, J.-M. Gulian, G. Laurent-Tabusse, Biochimie 58 (1976) 1071–1082.

[48] T. Lund, J. Vanngard, Chem. Phys. 42 (1965) 2979–2980.

[49] H.R. Gersmann, J.D. Swalen, J. Chem. Phys. 36 (1962) 3221–3233.

[50] a) J.R. Pilbrow, M.E. Winfield, Mol. Phys. 25 (1973) 1073–1092;
b) M.F. Corrigan, K.S. Murray, B.O. Weat, J.R. Pilbrow, Aust. J. Chem. 30 (1977) 2455–2463.

[51] M. Ferraroni, R. Gaspari, A. Scozzafava, A. Cavalli, C.T. Supuran, J. Enzyme Inhib. Med. Chem. 33 (2018) 999–1005.

[52] I. Zawisza, M. Rózga, J. Poznański, W. Bal, J. Inorg. Biochem. 129 (2013) 58–61.

[53] J. Nagaj, K. Stokowa-Sołtys, E. Kurowska, T. Frączyk, M. Jeżowska-Bojczuk, W. Bal, Inorg. Chem. 52 (2013) 13927–13933.

[54] S. Niranjanakumari, J.C. Kurz, C.A. Fierke, Nucleic Acids Res. 26 (1998) 3090–3096.

[55] P. Wingfield, Curr. Protoc. Protein Sci. 88 (2003) 6.14.1–6.14.3.

[56] H. Song, D.L. Wilson, E.R. Farquhar, E.A. Lewis, J.P. Emerson, Inorg. Chem. 51 (2012) 11098–11105.

[57] H. Irving, R.J.P. Williams, Nature 162 (1948) 746–747.

[58] L. Alderighi, P. Gans, A. Ienco, D. Peters, A. Sabatini, A. Vacca, Coord. Chem. Rev. 184 (1999) 311–318.

[59] P. Bergsten, G. Amitai, J. Kehrl, K.R. Dhariwal, H.G. Klein, M. Levine, J. Biol. Chem. 265 (1990) 2584–2587.

[60] K.K. Millis, K.H. Weaver, D.L. Rabenstein, J. Org. Chem. 58 (1993) 4144–4146.

[61] J.Z. Pedersen, C. Steinkühler, U. Weser, G. Rotilio, Biometals 9 (1996) 3–9.

[62] W.S. Postal, E.J. Vogel, C.M. Young, F.T. Greenaway, J. Inorg. Biochem. 25 (1985) 25–33.

[63] K. Miyoshi, Y. Sugiura, K. Ishizu, Y. Iitaka, H. Nakamura, J. Am. Chem. Soc. 102 (1980) 6130–6136.

[64] G. Formicka-Kozłowska, H. Kozłowski, B. Jeżowska-Trzebiatowska, Acta Biochim. Pol. 26 (1979) 239–248.

[65] D. La Mendola, C. Giacomelli, E. Rizzarelli, Curr. Top. Med. Chem. 16 (2016) 3103–3130.

[66] Y. Hatori, S. Lutsenko, Antioxidants 5 (2016) 25.

[67] G. Calabrese, B. Morgan, J. Riemer, Antioxid. Redox Signal. 27 (2017) 1162–1177.

[68] J.-L. Roh, H. Jang, E.H. Kim, D. Shin, Antioxid. Redox Signal. 27 (2017) 106–114.

[69] G. Boysen, Chem. Res. Toxicol. 30 (2017) 1113–1116.

[70] Y. Hatori, S. Inouye, R. Akagi, IUBMB Life 69 (2017) 246–254.